JOURNAL OF CATALYSIS 130, 319–331 (1991)

Investigation of Iron Oxide–Chromia–Alumina Aerogels for the Selective Catalytic Reduction of Nitric Oxide by Ammonia

R. J. WILLEY, H. LAI, AND J. B. PERI

Department of Chemical Engineering, Northeastern University, 342 Snell Engineering, Boston, Massachusetts 02115

Received January 17, 1990; revised February 20, 1991

The selective catalytic reduction of nitric oxide by ammonia over iron oxide–chromia–alumina aerogels was studied over the temperature range of 423 to 750 K. The highest activities were observed for Fe/Cr/Al materials with a 60% conversion at 720 K for a reactor flow velocity of 1008 m^3/h-kg. Oxygen significantly enhanced the reaction rate as explained by a redox mechanism. Infrared characterization showed weak adsorption of nitric oxide on the preoxidized materials and quite strong adsorption on the reduced material; ammonia adsorption was strong on both oxidized and reduced materials. Observation of interaction between adsorbed nitric oxide and ammonia (when ammonia was added to reduced catalysts which held preadsorbed nitric oxide) provided insight into the reaction mechanism.

INTRODUCTION

The selective catalytic reduction (SCR) of nitric oxide by ammonia has been a suggested approach for the removal of nitric oxide from flue gases emitted from stationary sources. With legislation pending for lower NO_x emissions, evaluation of various materials for catalysis in SCR of NO is essential for understanding and optimizing future catalytic systems for this process. Oxygen, it is commonly observed, enhances the rate of reaction (*1–6*). The overall reaction stoichiometry in the presence of oxygen is

$$4\ NO + 4\ NH_3 + O_2 \rightarrow 4N_2 + 6\ H_2O. \quad (1)$$

When oxygen is not present, the overall reaction stoichiometry is

$$6\ NO + 4\ NH_3 \rightarrow 5\ N_2 + 6\ H_2O. \quad (2)$$

Many noble metal and mixed metal oxide materials have been investigated for Reactions 1 and 2. The classical work of Otto *et al.* described Reaction 2 over Pt (*7, 8*) and CuO catalysts (*9*). In terms of mixed metal oxides the two promising materials are vanadium oxide and iron oxide–chromium oxides on various supports. Bosch *et al.* (*10*) compared V_2O_5 on TiO_2 using continuous flow and pulse experiments. Nobe's group at UCLA (*2–4, 11*) has studied many oxide combinations. Notable is the work of Wong and Nobe (*11*) who looked at the reduction of NO with NH_3 in the presence of oxygen on V_2O_5, Cr_2O_3, Fe_2O_3, and mixtures of these metal oxides supported on TiO_2 and Al_2O_3. Chromia and chromia supported on alumina have been studied by Niiyama *et al.* (*12, 13*) who reported two maxima in reactivity at 9.3% Cr content and 100% Cr. Also, N_2O was produced under certain conditions as given by the stoichiometric equation

$$4\ NO + 2\ NH_3 \rightarrow 2\ N_2 + N_2O + 3\ H_2O. \quad (3)$$

SCR of NO has been reported for iron oxide supported on an alumina (*3, 11*) and titania (*5*). The combination of iron oxide and chromia has been investigated (*3, 6*). Ratios of Fe/Cr of 5 to 1 and 4 to 1 were used in these investigations. The first use of aerogel catalysts in the SCR of NO was by Willey *et al.* (*14*). The most active aerogel

0021-9517/91 $3.00

was a 4:1 Fe:Cr alumina aerogel synthesized as described by Teichner *et al.* (*15*).

Infrared studies on the adsorption of nitric oxide and ammonia on oxides and mixed oxide materials abound (Peri and King (*16, 17*); Kugler *et al.* (*18*), and Busca and Lorenzelli (*19*)). Infrared has been used by Takagi *et al.* to investigate the role of oxygen in SCR of NO over V_2O_5 catalysts (*20*). They concluded that ammonia adsorbed as NH_4^+ and that NO in the presence of O_2 adsorbed as NO_2(ad). These two surface species then reacted to form N_2 and H_2O. Work by Katzer (*21*) and Gland and Korchak (*22*), on the other hand, suggests the reaction mechanism is between an adsorbed NH_2 and adsorbed molecular NO species on Pt and supported Pt catalysts.

Aerogel materials are ideal for fundamental studies involved infrared spectroscopy because of their typically high surface areas and relatively low scattering losses. Further, the flexibility in their composition aids in systematic study. Therefore, infrared spectroscopy was used to investigate the nature of active sites for SCR on iron oxide and chromia on alumina aerogels.

EXPERIMENTAL

Synthesis of Iron Oxide–Chromia–Alumina Aerogels

The synthesis of iron oxide–chromia–alumina aerogels required five steps. Two separate solutions were developed. The first consisted of 12.5 wt% aluminum tri-sec-butoxide in sec-butanol. The second was made by mixing 0.5 wt% chromium acetylacetonate and 0.5% ferric acetylacetonate in methanol in specific proportions depending upon the aerogel made. The amount of water added to the second mixture was 1.2 times the stoichiometric amount required to hydrolyze the ferric and chromium acetylacetonates and aluminum tri-sec-butoxide to their respective hydroxides.

Solution 2 was then poured slowly (over a period of 1 min) into a rapidly agitated Solution 1. An aluminum methoxide gel formed immediately. Mixing was continued for another 5–15 min. The product was then placed into a Pyrex glass-liner which was then put into an autoclave and heated at about 2°C per min until the critical temperature of butanol (260°C) was reached. At this stage, the pressure was relieved while the temperature was held above the critical temperature. Finally, after the autoclave had been depressurized, it was purged with nitrogen and cooled to room temperature. The resultant aerogel was removed from the autoclave and stored at room temperature in glass jars until pretreatment or characterization.

Table 1 gives the composition and characteristics of the iron oxide–chromia–alumina aerogels investigated. The aerogels were as follows: (1) TTZ-4 with a combination of iron oxide–chromia–alumina, (2) TTZ-5 with iron oxide-alumina and, (3) TTZ-6 with chromia–alumina. These compositions were prepared in order to separate the influence of iron oxide and chromia on an alumina support. The surface areas and pore size distributions are for samples pretreated with oxygen at 500°C for a period of 2 h.

All materials were pretreated in flowing oxygen (for oxidized aerogel) or hydrogen (for reduced aerogel) at 500°C for a period of 2 h before testing in a separate flow reactor. Care was taken to make sure that hydrogen was not contacted with oxygen or air by flushing with helium for 15 min before and after activation. The resultant colors of the materials depended on the pretreatment. Table 1 shows the colors observed after the pretreatment. The infrared characterization section of this paper goes into further detail regarding the state of the metallic ions dependent upon pretreatment.

Infrared Characterization

Infrared characterization was carried out with either a Perkin–Elmer Model 580A or a Perkin–Elmer Model 1320 infrared spectrometer. A specially constructed cell, similar to that shown in Peri (*23*) with sodium chloride windows, allowed a sample to be

TABLE 1

Composition and Characteristics of Iron Oxide–Chromia–Alumina Aerogels Investigated

NU i.d	Metallic atomic ratios			Surface area[a] (m^2)	Peaks in pore size distribution[b] (nm)	Color observed after pretreatment oxidation	Reduction
	Fe	Cr	Al				
TTZ-4	0.08	0.02	0.90	500	3.4, 8.5	Reddish brown	Black
TTZ-5	0.082	—	0.908	518	1.8, 4.7	Reddish brown	Black
TTZ-6	—	0.022	0.978	366	1.8, 8.7	Yellow	Gray
JSR-4	—	—	1.00	412	1.8, 6.1	White	

[a] BET surface area by N_2 adsorption.

[b] Pore size distribution using N_2 adsorption analyzed by the Barrett, Joyner, and Halenda method.

raised (and then lowered again) from the infrared beam to a quartz tube furnace for calcination or reduction pretreatment and high temperature adsorption of probe molecules. The cell was connected to a vacuum manifold system which could supply nitric oxide, carbon dioxide, carbon monoxide, ammonia, and hydrogen. An isotopically labeled nitric oxide, ^{15}NO, was also used.

All chemicals used were dried and freed of permanent gases by vacuum distillation. Nitric oxide was vacuum distilled before use and carbon monoxide was pretreated by passage through an alumina adsorption bed. Hydrogen was purified by passage through a trap containing activated charcoal and alumina, cooled with liquid nitrogen.

The aerogels were formed into transparent disks by compressing material which had been preheated in a quartz tube at 600°C in air for 1 h. Disks were made by placing 300 mg of aerogel powder is a 1.25-in.-diameter cylindrical stainless-steel die and compressing under a pressure of 2,000 lb/in^2 for 40 s. These were then cut to fit a sample holder which was used in the IR cell.

Once in the IR cell, the disk was calcined in 200 Torr of air at 500°C for 1 h and dried by evacuation for 15 min. The disk was then cooled to room temperature and several infrared scans made. Depending upon the particular experiment, NO, NH_3, or CO_2 was then admitted to the cell and additional infrared scans made. The disk was then raised into the furnace and reduced in hydrogen at (50 Torr) for 1 h at 500°C. Spectral data were then digitized (PE 1320) or directly computerized (PE 580) which allowed the subtraction of background scans for the figures shown below.

Evaluation of Aerogels for Catalytic Activity in SCR of NO by NH_3

The catalysts were evaluated in a Pyrex reactor system which provided ease of filling and excellent contact between the gas and the catalyst bed. The reactor had an inside diameter of 22 mm. The catalyst behaved as a fluidized bed in the reactor. The reactor system consisted of a gas metering system which enabled a carrier gas, the either air or nitrogen (total flow of 58cc/s), to be doped with nitric oxide and ammonia. Inlet concentrations of NO and NH_3 were held constant at 2030 ± 50 ppm. The flow was split to an upstream bypass flow and a reactor flow. The reactor flow rate was 28 cc/s at NTP. The temperature range investigated was 423 to 723 K. Catalyst weight in the reactor was 100 mg in all experiments. The space velocity (NTP) was thus 1008 m^3/h-kg catalyst.

Product and feed analysis for NO concentrations were determined by a Thermal Electron Corporation Model 44 chemiluminescent analyzer. Determination of N_2O was done with an Antex Model 310 LP gas chromatograph. The column used in this

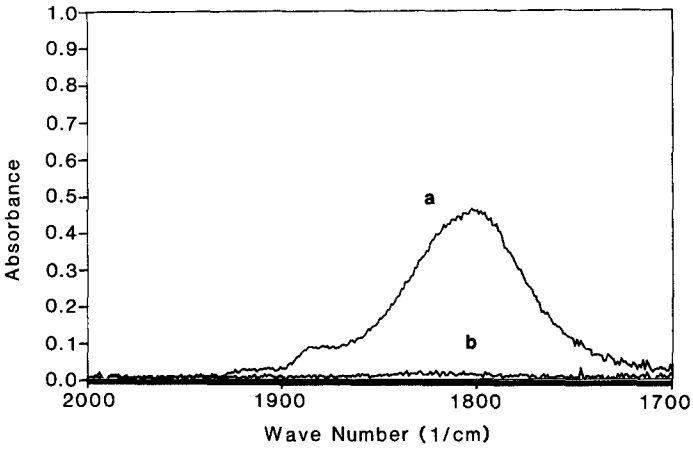

FIG. 1. Infrared spectra for NO adsorbed on oxidized iron oxide–alumina aerogel. (a) 3.2 Torr NO; (b) after evac. at 200°C for 15 min.

chromatograph was a Porapak QS of 1/4 in. o.d. and 8 ft in length.

The reactor was heated in a three-zone Lindberg furnace. Air or nitrogen with nitric oxide and ammonia added was flowed over the catalyst. The reactor started at a temperature of 150°C. Checks were made to make sure that no conversion was observed at low temperatures (150°C). The temperature was then increased approximately 3°C per minute. As the temperature rose, ppm concentration reading from the chemiluminescent analyzer (which monitored the reactor outlet stream) and reactor temperature were acquired by a microcomputer (IBM-XT) equipped with a Metrabyte DASH-16 A/D converter. Software called Lotus Measure (Lotus Corporation) was used to acquire data every 5 s as temperature increased. Most catalysts were run three times to ensure that results were repeatable and catalysts stable. A nitrogen cylinder was used as the source of gas when nitrogen was substituted for air.

RESULTS AND DISCUSSION

Infrared Characterization

Typical spectra observed when nitric oxide was adsorbed on oxidized iron oxide–alumina aerogel are shown in Fig. 1. Figure 1 displays a major band at 1810 cm^{-1} and two small shoulders at 1880 cm^{-1} and 1910 cm^{-1}. These bands are caused by one or two nitric oxide molecules held by exposed Fe^{+3} atoms. When ^{15}NO was held adsorbed on the materials, the bands were similar in appearance, but shifted by 35 cm^{-1} to a lower frequency. The adsorbed NO was held fairly weakly because, as indicated in Fig. 1, the bands disappeared after heating at 200°C for 15 min.

Adsorption of nitric oxide onto reduced iron oxide–alumina aerogel gave a very strong band at 1805 cm^{-1}. This nitric oxide was more difficult to remove than the nitric oxide adsorbed on oxidized iron as shown in Fig. 2. A possible explanation is that nitric oxide accepts an electron from the iron atom to form a bond, and Fe^{+2} donates such an electron more easily than Fe^{+3}. Therefore, the Fe–NO bond on reduced iron (which probably exposes Fe^{2+} ions) is stronger than on oxidized iron (where on Fe^{3+} is exposed). The existence of significant numbers of exposed Fe° sites on the reduced iron oxide–alumina aerogel seems unlikely, and, if such Fe° sites were originally produced by H_2 reduction, they would probably be quickly reoxidized by NO.

Ammonia adsorption onto oxidized iron

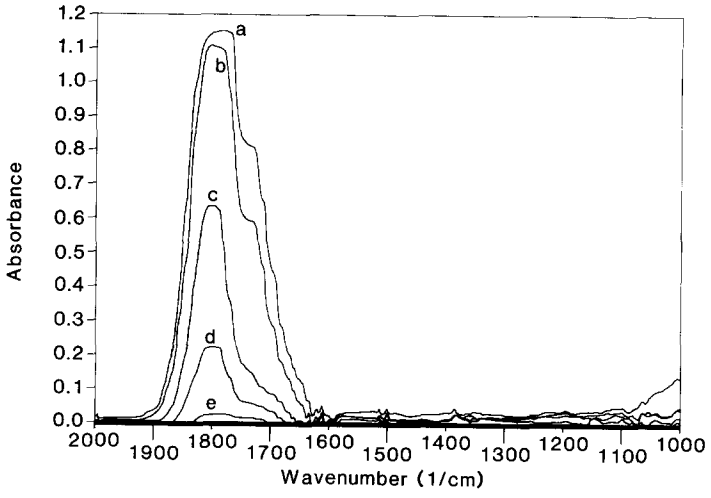

FIG. 2. Infrared spectra for NO adsorbed on a reduced iron oxide–alumina aerogel. (a) 0.3 Torr of NO; (b) after evac. at RT; (c) evac. 200°C for 5 min; (d) evac. 250°C for 5 min; (e) evac. 300°C for 5 min.

oxide–alumina aerogel is shown in Fig. 3. Strong adsorption is displayed with a broad-band at 1210 cm^{-1} which is probably the combination of several bands for the symmetric stretch of NH_3. Upon heating, this band shifts to represent strongly held NH_3 with a peak centered at 1260 cm^{-1}. A peak at 1610 is also seen representing NH_3 adsorption onto a Lewis acid site (Fe^{+3}). Ammonia is also strongly adsorbed onto the reduced iron oxide–alumina (spectra not shown). Species were seen on the surface even after heating at 350°C for 5 min.

Several IR experiments involved adsorption of NO and NH_3 on a reduced iron oxide–alumina surface. In one experiment, 2.0

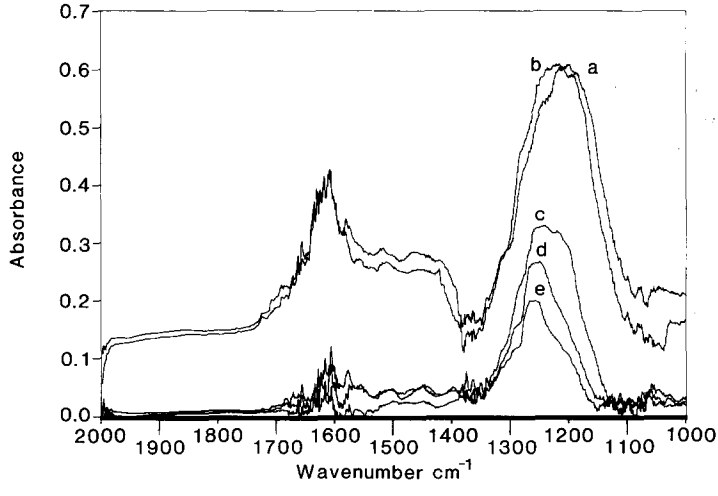

FIG. 3. Infrared spectra for NH_3 adsorbed on oxidized iron oxide–alumina aerogel. (a) 0.3 Torr NH_3; (b) evac. at RT for 5 min; (c) evac. 200°C for 5 min; (d) evac. 250°C for 5 min; (e) evac. 300°C for 5 min.

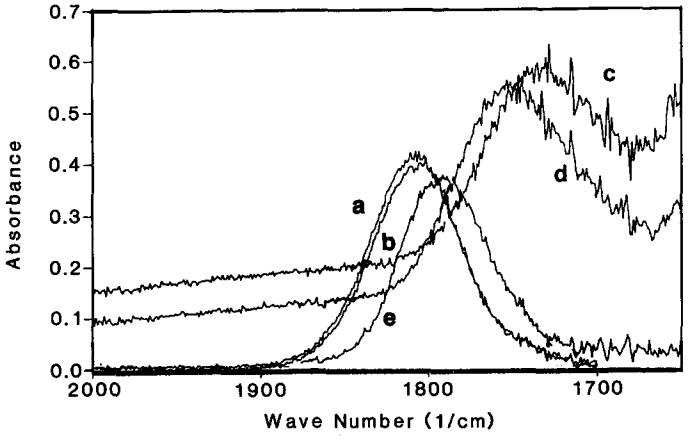

FIG. 4. Infrared spectra for adsorbed NO followed by adsorption of NH_3 on reduced iron oxide–alumina aerogel. (a) 3.7 Torr NO; (b) evac. at 200°C for 5 min; (c) add 2 Torr NH_3; (d) evac. at RT for 20 min; (e) evac. at 200°C for 10 min.

Torr of NO was added, followed by evacuation at 200°C for 5 min followed by the adsorption of 2.0 Torr of NH_3. Figure 4 shows the spectra obtained. In spectrum C, Fig. 4, the NO band has shifted to a lower frequency of about 1730 cm^{-1} after NH_3 was admitted. With a partial evacuation removing some of the adsorbed gases the nitric oxide band moved slightly back toward its original (1805 cm^{-1}) frequency (curve D). When the sample was heated at 200°C under vacuum, the nitric oxide band was restored to nearly its original shape and frequency of 1805 cm^{-1}. This shift in frequency of the nitric oxide band to a lower frequency when ammonia is adsorbed shows a direct interaction of NO and NH_3 occurring on the surface.

Figure 5 demonstrates an experiment where NH_3 and NO were coadsorbed onto reduced iron oxide–alumina. The spectra display two very broad bands, one initially centered at 1720 cm^{-1} representing NO adsorption (which is shifted) and a second located at 1210 cm^{-1} representing NH_3 adsorption. After a room temperature evacuation, we see that the species removed are those causing lower frequency NO and NH_3 bands. Upon heating to 150°C (near reaction temperature) more of these frequency shifted species are removed. Isolated NO and NH_3 is removed upon heating at higher temperatures. Figure 5 suggests that the species removed is reactive NO interacting with NH_3 on the surface. The rate of reaction begins to take off around 225°C. The surface could thus be in a semi-frozen (prereaction) condition below 225°C. Reactive species on the surface may be seen with infrared. Species seen in the infrared after evacuation at temperatures above 250°C are probably not related to the reaction since the reaction rate is quite rapid and 5 min. of heating at 250°C should clear the surface of all species related to the SCR reaction. Heating at higher temperatures resulted in the removal of isolated NO and NH_3.

An experiment in which CO_2 was adsorbed onto the surface of oxidized iron oxide–alumina was performed. Upon adsorption of CO_2, several bands were seen including weak adsorption of CO_2 onto alumina (band at 1860 cm^{-1}, spectra not shown). The spectra shown in Fig. 6 are for after CO_2 plus a 5-min evacuation and after subsequent adsorption of NH_3. Figure 6 shows the existence of several CO_2 species (curve a) on the surface. The peaks at 1760 and 1230 cm^{-1} are related to the adsorption onto $Fe^{+3}O^{2-}$ as bidentate carbonate as described by Little (*25*). When ammonia is added (spectrum b) CO_2 is displaced. The difference spectrum, spectrum c, shows that

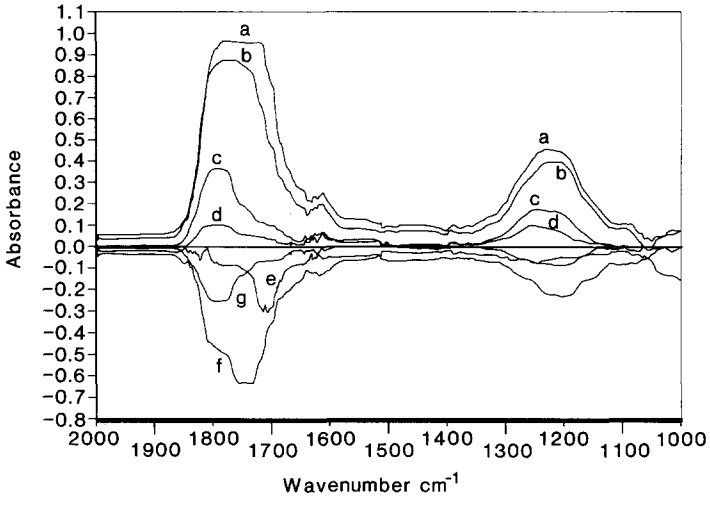

FIG. 5. Infrared and difference spectra for coadsorption of NO and NH_3 onto reduced iron oxide–alumina followed by heating. (a) Evac. at RT; (b) 150°C 5 min; (c) 200°C 5 min; (d) 250°C 5 min; (e) species removed after heating to 150°C (b–a); (f) species removed 150 to 200°C (c–b); (g) species removed 200 to 250°C (d–c).

the bidentate carbonate species is displaced. This suggests that ammonia adsorbs onto the oxidized surface as follows:

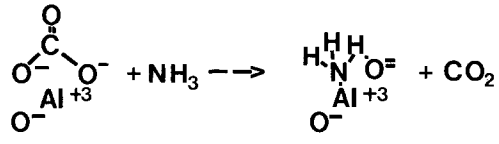

Adsorption of this type, where ion–dipole interaction is combined with hydrogen bonding, was postulated by Blyholder and Richardson (*26*) to explain the spectra of NH_3 strongly adsorbed on activated alpha Fe_2O_3. The essential configuration of NH_3 is clearly retained whether adsorption occurs by interaction of NH_3 with pure Lewis acid sites or with acid–base sites which can also accept H-bonding. If the surface is

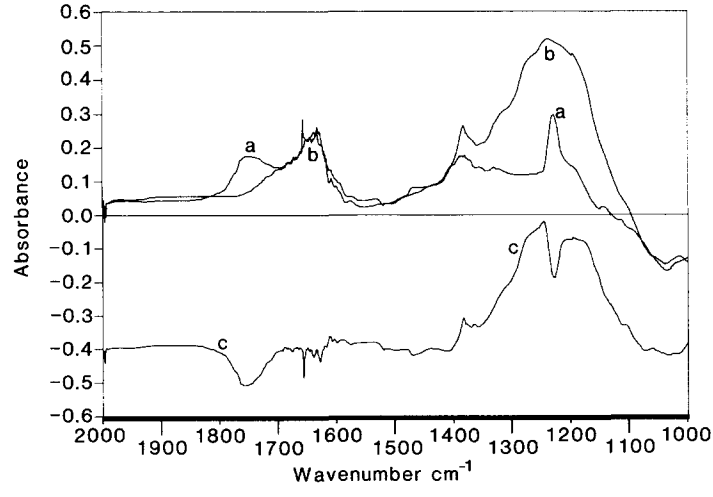

FIG. 6. Infrared spectra of CO_2 followed by NH_3 onto oxidized iron oxide–alumina. (a) +2 Torr CO_2 followed by evac. at RT for 5 min; (b) +1 Torr NH_3; (c) difference between b and a plus an offset of −0.4.

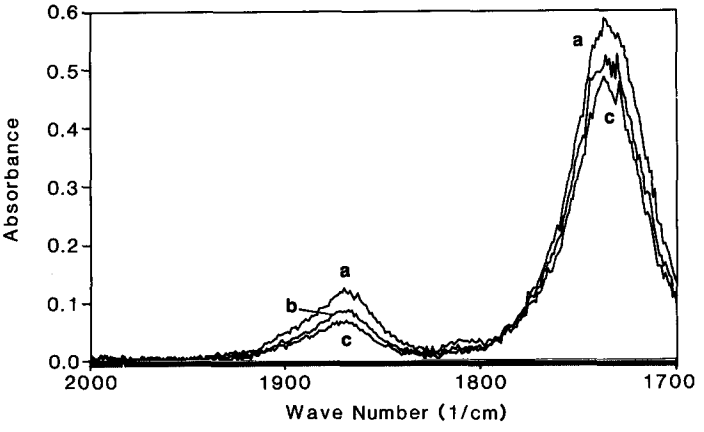

FIG. 7. Infrared spectra for NO adsorbed on reduced chromia–alumina aerogel. (a) 9.0 Torr of NO; (b) evac. at RT for 5 min; (c) evac. at RT for 10 min.

heated the H can detach from the ammonia and an electron is donated to the Fe^{3+} to form Fe^{2+}. This site can then serve as a host site for NO adsorption.

The adsorption of NO on oxidized chromia–alumina aerogel catalyst produced no significant bands on the oxidized chromia. This result agrees with those of Peri (*17*) and Zecchina *et al.* (*27*). On reduced chromia, two strong nitric oxide bands were observed at 1868 and 1737 cm^{-1}. These two bands, shown in Fig. 7, are assigned to the dinitrosyl $-Cr(NO)_2$. The addition of ammonia to this material demonstrates an interaction of adsorbed nitric oxide with adsorbed ammonia on reduced chromia alumina, as shown in Fig. 8. The NO band at 1868 cm^{-1} disappeared and the band at 1731 cm^{-1} was shifted to a lower frequency. The consequences of this shifting could be seen by adding more NO with ammonia adsorbed. The two bands were shifted to 1855 and 1722 cm^{-1}. Peri (*17*) also reported similar results.

The peaks seen with NO adsorbed on oxidized iron oxide–alumina aerogels were also observed for NO on oxidized iron oxide–chromia–alumina aerogels. A similar shift was observed when ammonia was added to the materials.

When NO was added to reduced iron oxide–chromia–alumina two major bands were again observed at 1805 cm^{-1} (Fe) and 1735 cm^{-1} (Cr). Figure 9 shows spectra of NO adsorbed on reduced iron oxide–chromia–alumina. These spectra show that after evacuation at 200°C most of the NO on the chromia had disappeared (spectrum B) and the more strongly adsorbed NO on the iron oxide remained. Spectrum D shows that after the addition of ammonia, the NO band again shifted indicating interaction of adsorbed NO with adsorbed NH_3 on the surface. Upon heating at 200°C the NO band again gradually returned to its original position of 1805 of cm^{-1} (spectrum F).

Evaluation of Catalytic Activity

Influence of oxygen. The influence of oxygen on the rate of reduction of nitric oxide by ammonia can be clearly seen in Figs. 10 and 11. Figure 10 shows that the maximum conversion of about 9% occurred at the maximum temperature investigated of 450°C for Runs 1 and 2 which had nitrogen as the carrier. In Run 3, a carrier gas change was made to air. The conversion of NO jumped from 9% to almost 45% at 450°C. The influence of oxygen can also be seen in Fig. 11, where the temperature was held constant at 460°C and the conversion was constant for a period of 20 min at 43% (Run

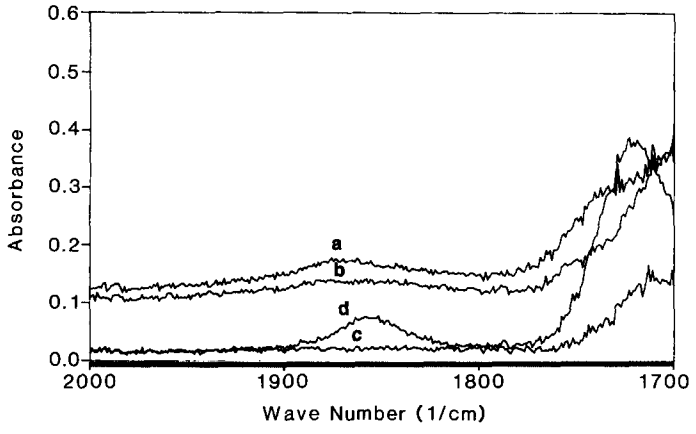

FIG. 8. Infrared spectra for adsorbed NO with concurrent NH_3 adsorption on reduced chromia–alumina aerogel. (a) 1.3 Torr NH_3 added after NO adsorption; (b) evac. at RT for 5 min; (c) evac. at 200°C for 5 min; (d) readmission of 7 Torr NO.

A). When the carrier gas was switched over to nitrogen, the conversion declined steadily from 43 to about 10% over a period of about 20 min. This indicates that the catalyst surface supplies oxygen in part of the mechanism and that surface oxygen can be depleted when the carrier gas no longer contains gaseous oxygen.

Evaluation of the chromia–alumina aerogels and the iron oxide–chromia–alumina aerogels showed similar behavior when the carrier gas was nitrogen versus air, with conversions of about 10% with nitrogen and as high as 60% with air at the conditions investigated. Stability of the iron oxide–chromia–alumina aerogel is shown in Fig. 12. Three runs are shown in which the conversion versus the temperature curves

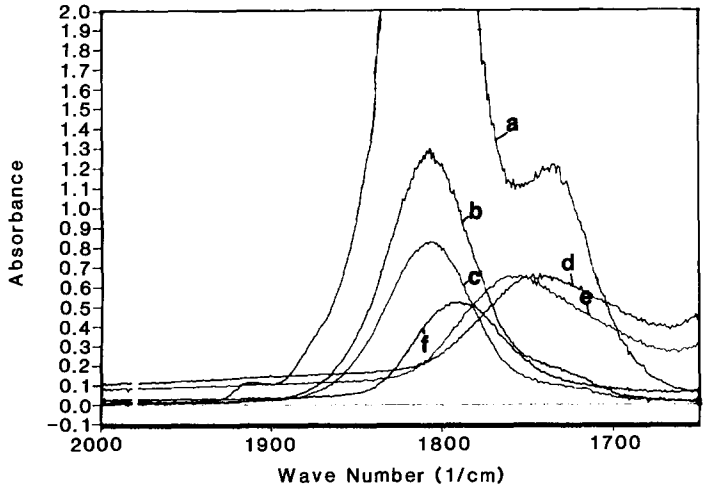

FIG. 9. Infrared spectra for adsorbed NO with concurrent NH_3 on reduced iron oxide–chromia–alumina aerogel. (a) 4.8 Torr of NO followed by evac. at RT for 40 min; (b) evac. at 200°C for 5 min; (c) evac at 200°C for 10 min; (d) add 1.9 Torr of NH_3; (e) evac. at RT for 10 min; (f) evac. at 200°C for 5 min.

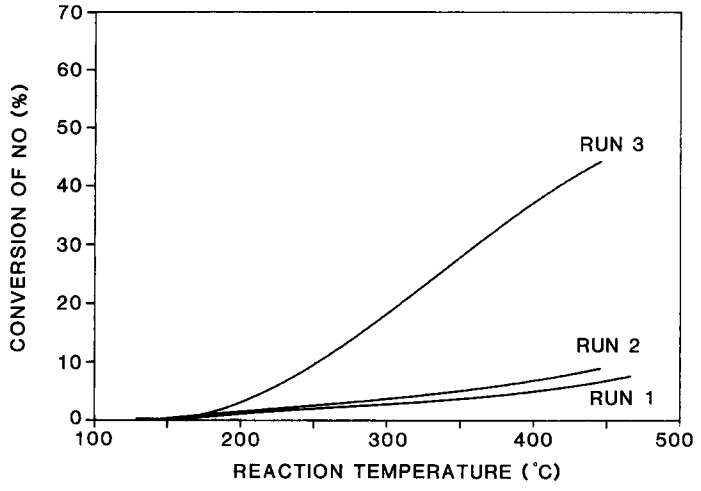

FIG. 10. Activity of a reduced iron oxide–alumina aerogel for the SCR of NO by NH_3 in N_2 or air. Runs 1 and 2 nitrogen carrier. Run 3, air carrier.

are nearly identical. Also, N_2O was detected only for the chromia–alumina aerogel catalyst in a temperature range of 380 to 475°C. The amount of N_2O was about 25% of the NO converted to N_2 or N_2O.

The Nature of the Active Site

Table 2 summarizes the results in terms of the specific rates for the selective catalytic reduction of nitric oxide by ammonia per gram of catalyst and per gram of Fe + Cr. The overall rates observed for the iron oxide–chromia–alumina aerogel could be approximated by the addition of the rate found for the chromia–alumina aerogel plus the rate for the iron oxide–alumina aerogel. To demonstrate the additive effect, the predicted intrinsic rate at 427°C for the oxidized Fe/Cr/Al (0.8 Fe/0.2 Cr) aerogel in an air carrier would be roughly 0.8 times 82 (the

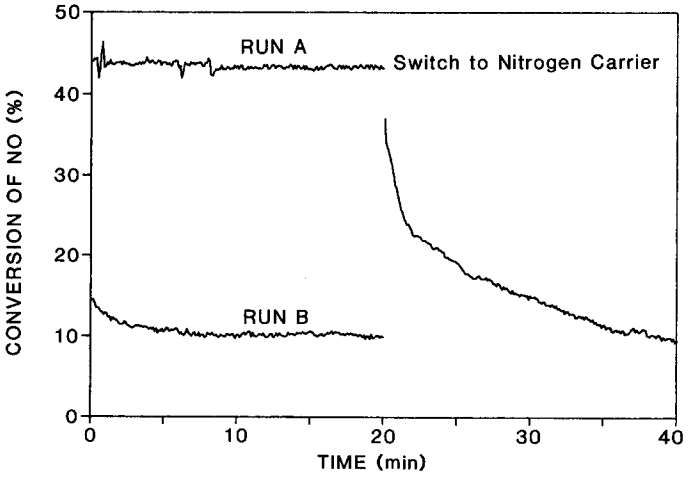

FIG. 11. Activity of an oxidized iron oxide–alumina aerogel for the SCR of NO by NH_3 at 733 K. Run A, carrier gas switched from air to nitrogen at 20 min into the run. Run B, nitrogen carrier gas.

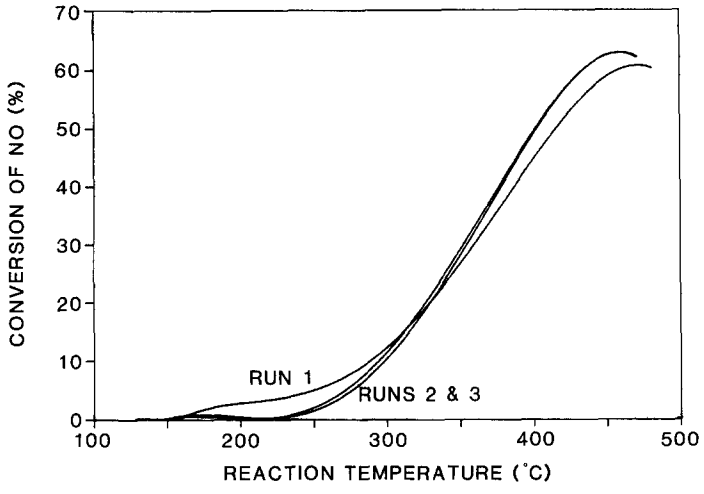

FIG. 12. Activity of an oxidized iron oxide–chromia–alumina aerogel for the SCR of NO by NH_3 in air.

average rate for Fe/Al) plus 0.2 times 500 (the average rate for Cr/Al) for a value of 166 μmol/g (Fe + Cr) s. The observed average was 132 μmol/g (Fe + Cr) s. Table 2 further demonstrates that chromia is a very powerful site for the reduction of nitric oxide by ammonia. Intrinsic rates were observed at 500 μmol/g Cr s for this catalyst compared to 82 μmol/g Fe for an iron oxide–alumina catalyst. Thus the mixed iron oxide–chromia–alumina aerogels simply showed an additive effect as opposed to a complex surface interaction between sites at these site concentrations.

The results also show that the reduced catalyst in the presence of air could give

TABLE 2

Summary of Results: Specific Rate for the SCR of NO by NH_3 per Gram of Catalyst Temperature 427°C (700 K)

	Carrier gas	μmol/g-s	μmol/g (Fe + Cr)-s
		Fe/Cr/Al	
Oxidized	Air	13.5	132
	Air	13.5	132
Reduced	Air	14.1	138
	N_2	2.3	22
		Fe/Al	
Oxidized	Air	6.8	78
	Air	7.5	86
Reduced	Air	9.7	112
	N_2	1.4	16
		Cr/al	
Oxidized	Air	11.2	503
	Air	11.1	498
Reduced	Air	10.4	467
	N_2	1.9	85

higher rates of reduction at low temperatures under certain transient conditions. For example, a reduced Fe/Cr/Al where air was the carrier had a rate of 3.1 μmol/g s. at 227°C. This is about three times higher than the rate on the oxidized Fe–Cr–Al sample (0.85 μmol/g sec). Similar results were observed for the chromia–alumina aerogel for which the reduced catalyst with air as a carrier again had an activity of 3.1 μmol/g s 227°C compared to 0.80 μmol/g s for oxidized catalyst. When the runs were repeated, the rates would approach those observed for the oxidized catalyst. This suggests that the optimum active site on the catalyst is found on a partially reduced type surface. In other words a redox mechanism applies and the maximum rate is observed when some combination of reduced and oxidized sites coexist on the surface.

Mechanistic Discussion

Based on the results of the infrared characterization and reaction analysis the following redox mechanism is suggested:

Ammonia adsorption onto a fully oxidized site

$$NH_3 + M^{+3}O^{2-} \rightleftarrows NH_3M^{3+}O^{2-} \quad (1)$$

Adsorbed ammonia can then reduce the site via a hydrogen transfer:

$$NH_3\ M^{3+}O^{2-} \rightleftarrows NH_2\text{-}M^{2+}\overset{H}{\overset{|}{O}}^{-} \quad (2)$$

Nitric oxide adsorption onto the surface

$$NO + NH_2\text{-}M^{2+}\overset{H}{\overset{|}{O}}^{-} \rightarrow NH_2\text{-}M^{2+}\overset{NO\,H}{\overset{|\quad|}{O}}^{-} \quad (3)$$

Then surface reactions to create water and nitrogen:

The decomposition of species shown in Step 3

$$NH_2\text{-}M^{2+}\overset{NO\,H}{\overset{|\quad|}{O}}^{-} \rightarrow M^{2+}\overset{H}{\overset{|}{O}}^{-} + N_2 + H_2O \quad (4)$$

Finally reoxidation of surface by oxygen.

$$4\ M^{2+}\overset{H}{\overset{|}{O}}^{-} + O_2 \rightarrow 4\ M^{+3}O^{2-} + 2\ H_2O \quad (5)$$

$$2\ Cr^{2+}\overset{H}{\overset{|}{O}} + 2NO \rightarrow 2\ Cr^{+3}O^{2-} + H_2O + N_2O \quad (6)$$

The transition $M^{3+}O^{2-} \rightarrow M^{2+}O^{-}$ is a reduction in which surface hydrogen reduces the oxide one valence state. The transition $M^{2+}O^{-} \rightarrow M^{3+}O^{2-}$ is an oxidation in which oxygen removes surface hydrogen.

Step 1 in the above mechanism represents adsorption of ammonia onto exposed (coordinatively unsaturated) oxidized metal sites. The infrared results discussed above suggest that NH_3 can be held on the same type of site as the bidentate carbonate. Step 3 suggests that adsorbed nitric oxide is coordinated with a neighboring ammonia on the same site because the infrared results showed a frequency shift in the nitric oxide band when ammonia was adsorbed. Adjacent M^{2+} sites could, however, also permit interaction between adsorbed NO and NH_3 leading to frequency shift of the NO band. Step 4 represents the combination of NO with NH_2 to form N_2 and H_2O. Infrared work reported above supports that NO and NH_3 are held together on the same site (or very close adjacent sites) and that they are readily removed at 250°C (near the temperature where reaction rates begin to increase rapidly). A reduced site results when nitrogen and water leave the surface. The reduced surface can be oxidized either by oxygen or nitric oxide from the gas phase. Since N_2O appeared only with chromia–alumina aerogels, chromia is the species shown in Step 6. The reason the rate declines when oxygen is not present is probably because the oxidizing species needed to regenerate the oxidized sites for NH_3 adsorption is no longer present in high enough concentrations. When oxygen is present, the rate limiting step is probably Step 4. When oxygen is not present in the reaction, the rate limiting

step is the removal of surface hydroxide due to the concentration of nitric oxide being so low (in the parts per million) that it does not rapidly reoxidize the catalyst.

The mechanism above can be compared to one predicted in Ref. (*6*). The primary difference is in Step 3 where the combination of NO and surface NH_2 occurs on the same site versus two neighboring sites, as is shown in Ref. (*6*). Thus resultant kinetic models will be different; one major difference being the description of the rate as a function of ammonia partial pressure. The mechanism above does not explain a rapid increase in rate followed by a gradual decline as ammonia partial pressure is increased (data shown in Ref. (*6*)). However, if ammonia competitively adsorbed on the site holding NH_2, then higher partial pressure of NH_3 would block NO adsorption and thus retard the rate as reported in Ref. (*6*). Other functionalities shown in Ref. (*6*) (NO adsorption described by a Frendulich isotherm, oxygen functionality of approximate $\frac{1}{4}$ power, and the slight retardation of rate when water partial pressure was increased) can be supported by the above mechanism. Perhaps, in the future we will attempt to derive a kinetic model from the above mechanism which can describe the wide range of data presented in Ref. (*6*).

ACKNOWLEDGMENTS

The authors acknowledge support through the Wm. O. DiPetro Young Professor Award and the Cabot Corporation Foundation. Also, Ms. Jian Ping Chen is acknowledged for her assistance on surface area and pore size distribution measurements. We also acknowledge the referee's very helpful comments made after the first review of this manuscript.

REFERENCES

1. Markvart, M., and Pour, V., *J. Catal.* **7,** 279 (1967).
2. Bauerle, G. L., Wu, S. C., and Nobe, K., *Ind. Eng. Chem. Prod. Res. Dev.* **14,** 268 (1975).
3. Wu, S. C., and Nobe, K., *Ind. Eng. Chem. Prod. Res. Dev.* **16,** 136 (1977).
4. Bauerle, G. L., Wu, S. C., and Nobe, K., *Ind. Eng. Chem. Prod. Res. Dev.* **17,** 117 (1978).
5. Kato, A., Matsuda, S., Nakajima, F., Imanari, M., and Watanabe, Y., *J. Phys. Chem.* **85,** 1710 (1981).
6. Willey, R. J., Eldridge, J. W., and Kittrell, J. R., *Ind. Eng. Chem. Prod. Res. Dev.* **24,** 226 (1985).
7. Otto, K., Shelef, M., and Kummer, J. T., *J. Phys. Chem.* **74,** 2690 (1970).
8. Otto, K., Shelef, M., and Kummer, J. T. *J. Phys. Chem.* **75,** 875 (1971).
9. Otto, K., and Shelef, M., *J. Phys. Chem.* **76,** 37 (1972).
10. Bosch, H., Janssen, F. J. J. G., van der Kerkhof, F. M. G., Oldenziel, J., van Ommen, J. G., and Ross, J. R. H., *Appl. Catal.* **25,** 239 (1986).
11. Wong, W. C., and Nobe, K., *Ind. Eng. Chem. Prod. Res. Dev.* **25,** 179 (1986).
12. Niiyama, H., Murata, K., Ebitani, A., and Echigoya, E., *J. Catal.* **48,** 194 (1977).
13. Niiyama, H., Murata, K., Ebitani, A., and Echigoya, E., *J. Catal.* **48,** 201 (1977).
14. Willey, R. J., Olmstead, J., Djuhadi, Y., and Teichner, S. J., *Mater. Res. Soc. Symp. Proc.* **3,** 359 (1988).
15. Teichner, S. J., Nicolaon, G. A., Vicarini, M. A., and Gardes, G., *Adv. Colloid Interface Sci.* **5,** 245 (1976).
16. King, D. L., and Peri, J. B., *J. Catal.* **79,** 164 (1983).
17. Peri, J. B., *J. Phys. Chem.* **78,** 588 (1974).
18. Kuglar, E. L., Kadlet, A. B., and Gryder, J. W., *J. Catal.* **41,** 72 (1976).
19. Busca, G., and Lorenzelli, V., *J. Catal.* **72,** 303 (1981).
20. Takagi, M., Kawai, T., Mitsuyuki, S., Onishi, T., and Tamaru, K., *J. Catal.* **50,** 441 (1977).
21. Katzer J. R., *in* "The Catalytic Chemistry of Nitrogen Oxides" (R. L. Klimisch and J. G. Larson, Eds.), pp. 133–166. Plenum, New York, 1975.
22. Gland J. L., and Korchak, V. N., *J. Catal.* **55,** 324 (1978).
23. Peri, J. B., *in* "Catalysis" (J. R. Anderson and M. Boudard, Eds.), Vol. 5, Chap. 3, pp. 172–219. Springer-Verlag, Berlin, New York, 1984.
24. Peri, J. B., *J. Phys. Chem.* **70,** 3168 (1966).
25. Little, L. H., "Infrared Spectra of Adsorbed Species," p. 76. Academic Press, New York, 1966.
26. Blyholder, G., and Richardson, E. A., *J. Phys. Chem.* **66,** 2597, 1962.
27. Zecchina, A., Garonne, E., Morterra, C., and Coluccia, S., *J. Phys. Chem.* **79,** 978 (1975).